Impact Of The Effective Conducting Path Effect (ECPE) On The Convergence Of The Evanescent And The Polynomial Models: Applied To The Submicronic MOSFET

A. BOUZIANE, A. AOUAJ and A. NOUAçRY

Laboratoire de physique de la matière et nanotechnologie, Faculté des Sciences et Techniques, Université Sultan Moulay Slimane, BP523 Beni-Mellal, CP23000, Morocco.

Abstract: We present a comparative study of submicronic MOSFET characteristics using analytic models of electrostatic potential in the channel. We are particularly interested in the surface potential, threshold voltage, swing and DIBL using the polynomial model with and without ECPE and the evanescent model to analytically express the electrostatic potential. The results show a good agreement between the polynomial model including ECPE, the evanescent model and measures done by simulation tools.

Keywords: submicronic MOSFET; evanescent model; effective conducting path effect; DIBL and Swing.

I. Introduction

The CMOS technology with very large scale integrated (VLSI), due to its technological simplicity and its low cost, remains the principal technology of the Ultra-submicronic components functioning with low supplying tensions. The components miniaturization, generating unsatisfactory performances, has led searchers to figure out eventual possibilities to reduce short channel effects on the components performances [1-2]. The characteristic length λ, defined through the resolution of the 2D Poisson equation and relying on the transistor geometric parameters [3], represents one of the parameters characterizing the short channel effects. The decreasing of the characteristic length λ, through the MOSFET geometry changing such as SSR-MOSFET, DG-MOSFET and CG-MOSFET [3-4], has improved its performances.

In this paper, we develop the evanescent model to determine the surface potential, the threshold voltage, the DIBL and Swing for the submicronic MOSFET transistor. We compare these results with those obtained from the polynomial model of electrostatic potential with and without ECPE [5] and simulation measures [6-7-8 -9].

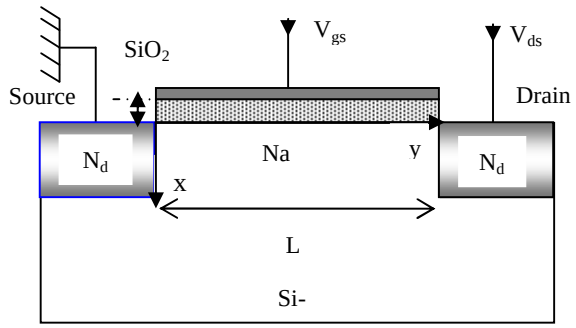

Figure1: Conventional MOSFET

II. Evanescent model

II-1. Surface potential and threshold voltage

The surface potential and the threshold voltage are deduced through the 2D Poisson equation neglecting beforehand the inversion charge in regard to that of the depletion. We define the channel length by L, the homogenous doping below the grid by Na and the silicon permittivity by ε_{si}.

In the evanescent model, the electrostatic potential is represented by $\varphi(x,y) = \varphi_1(x) + \varphi_2(x,y)$. $\varphi_1(x)$ is the solution of Poisson equation for a long channel and $\varphi_2(x,y)$ is the solution of the Laplace equation and contain the short channel effect.

$$\frac{d^2\varphi(x,y)}{dx^2} + \frac{d^2\varphi(x,y)}{dy^2} = \frac{qN_a}{\varepsilon_{si}} . \qquad (1)$$

The necessary boundary conditions of φ_1 and φ_2 to define $\varphi(x)$ are as follow:

For φ_1 :

$$-\varphi_1(x=0) = V_{SL} = \varphi_{gf} - \frac{qN_a T_{ox} x_m}{\varepsilon_{ox}}$$

$$-\frac{\partial\varphi_1}{\partial x}\Big)_{x=0} = \frac{C_{ox}}{\varepsilon_{si}}.(\varphi_1(0) - \varphi_{gf}) \qquad \text{where} \quad \varphi_{gf} = V_{Gs} - V_{FB}$$

V_{SL} represents the surface potential for a long channel, V_{GS} is the grid bias and V_{FB} is the flat band voltage. $x_m \left(= \left[\frac{2\varepsilon_{si}(2\phi_B - V_{BS})}{qN_a} \right]^{\frac{1}{2}} \right)$ is the maximum depletion region in the channel, $\phi_B \left(= \frac{KT}{q}.Ln\left(\frac{N_a}{n_i}\right) \right)$ is the Fermi potential in the channel and $C_{ox} \left(= \frac{\varepsilon_{ox}}{T_{ox}} \right)$ is the capacity of the grid oxide per surface unity.

For φ_2:

$$\begin{cases} \varphi_2(x, y=0) = V_{bi} - \varphi_1(x) & \left(\frac{\partial \varphi_2}{\partial x}\right)_{x=0} = \frac{C_{ox}}{\varepsilon_{si}}.\varphi_2(x=0, y) \\ \varphi_2(x, y=L) = V_{bi} + V_{ds} - \varphi_1(x) & \left(\frac{\partial \varphi_2}{\partial x}\right)_{x=0} = 0 \end{cases}$$

where $V_{bi} = \frac{kT}{q}.Ln\left(\frac{N_a.N_d}{n_i^2}\right)$ denotes the built-in voltage between the source/drain end, with the doping N_d, and silicon body and V_{ds} is the drain bias. T_{ox} is the oxide thickness.

$\varphi_s(y) = \varphi_1(0) + \varphi_2(0, y)$ is the surface potential of silicon (x=0) and write explicitly as follow:

$$\varphi_s(y) = V_{SL} + \left\{ (V_{bi} + V_{ds} - V_{SL}).\frac{\sinh(y/\lambda_e)}{\sinh(L/\lambda_e)} + (V_{bi} - V_{SL}).\frac{\sinh(\frac{L-y}{\lambda_e})}{\sinh(L/\lambda_e)} \right\}. \quad (2)$$

λ_e is the characteristic length of the evanescent model and verify the follow equality

$$\tan g\left(\frac{x_m}{\lambda_e}\right) - \frac{C_{ox}}{\varepsilon_{si}}\lambda_e = 0 . \quad (3)$$

Threshold voltage is defined as a grid voltage ($V_{GS} = V_{th}$) for $\varphi_s = 2\phi_B$. This leads to write V_{th} as follow:

$$V_{th} - V_{FB} = \frac{qN_a}{C_{ox}}.x_{\max} + \frac{\left\{ 2\phi_B - (V_{bi} + V_{ds}).\frac{\sinh(y/\lambda_e)}{\sinh(L/\lambda_e)} - V_{bi}.\frac{\sinh(\frac{L-y}{\lambda_e})}{\sinh(L/\lambda_e)} \right\}}{\left\{ 1 - \frac{\sinh(y/\lambda_e)}{\sinh(L/\lambda_e)} - \frac{\sinh(\frac{L-y}{\lambda_e})}{\sinh(L/\lambda_e)} \right\}} . \quad (4)$$

The gradient of threshold voltage is defined as $\Delta V_{th} = V_{th0} - V_{th}$ where $V_{th0} - V_{FB} = \frac{qN_a}{C_{ox}}.x_{\max} + 2\phi_B$ and V_{th0} denote the threshold voltage for a long channel MOSFET [8].

II-2. DIBL

In the MOSFET structures with short channel, the surface potential minimum increase with the drain voltage. Thus, the short channel effect is attributed to the penetration of the electric field line, of the drain-channel junction, in the channel resulting in the potential barrier lowering (DIBL). This leads to the decreasing of the threshold voltage.

The $\Re$ parameter defined by $\Re = \frac{\partial V_{th}}{\partial V_{ds}}$ evaluates the DIBL effect and written as

$$\Re = \frac{2\sinh^2(L/2\lambda_e)}{K_1}\left\{ -1 + \frac{K_2}{(K_2^2 - K_1K_3)^{1/2}} \right\} + \frac{V_{ds}}{\left(K_2^2 - K_1K_3\right)^{1/2}} . \quad (5)$$

where

$$K_1 = \sinh^2(L/\lambda_e) - 4\sinh^2(L/2\lambda_e)$$

$$K_2 = \left(2\phi_B - V_{bi}\right)\sinh^2(L/\lambda_e) - 2V_{ds}\sinh^2(L/2\lambda_e)$$

$$K_3 = \left(2\phi_B - V_{bi}\right)^2\sinh^2(L/\lambda_e) + V_{ds}^2$$

II-3. Swing

The subthreshold slope parameter, appealed Swing, is defined as the grid voltage that modifies the drain current under a threshold of a decade and written as $S = \frac{\partial V_{gs}}{\partial Ln(I_{ds})}$ where I_{ds} denotes the drain current.

Sean be written differently according to the minimum surface potential

$\varphi_{s\min}$: $S = Ln(10).\frac{\partial V_{gs}}{\partial \varphi_{s\min}}\frac{\partial \varphi_{s\min}}{\partial Log(I_{ds})}$. When the surface states are neglected, the drain current is proportional to $\exp\left(\frac{q\varphi_{s\min}}{KT}\right)$. This leads to write S as follows $S = \frac{kT}{q}.Ln(10).\frac{\partial V_{gs}}{\partial \varphi_{s\min}}$.

The determination of the minimum surface potential y_0 abscise allows to write the parameter S taking into consideration the short channel effect as

$$S = \frac{KT}{q}.Ln(10).\frac{\partial V_{gs}}{\partial V_{SL}}.\left(1 - \frac{\sinh(y_0/\lambda_e)}{\sinh(L/\lambda_e)} - \frac{\sinh((L-y_0)/\lambda_e)}{\sinh(L/\lambda_e)}\right)^{-1}$$

. (6)

The corrective term

$$\gamma_s = \left(1 - \frac{\sinh(y_0/\lambda_e)}{\sinh(L/\lambda_e)} - \frac{\sinh((L-y_0)/\lambda_e)}{\sinh(L/\lambda_e)}\right) \quad (7)$$

denotes the short channel effect [10].

$$\frac{\partial V_{gs}}{\partial V_{SL}} = 1 + \frac{C_{dep}}{C_{ox}} \quad (8)$$

illustrates undoubtedly the modulation of the surface potential for a long channel MOSFET caused by the grid bias.

Finally, the swing can be written as

$$S = \frac{KT}{q}.\log_{10}.\frac{1}{\gamma_s}.\left(1 + \frac{C_{dep}}{C_{ox}}\right). \quad (9)$$

where $C_{dep} = \frac{x_{\max}}{\varepsilon_{si}}$ denote the capacity of the depletion region in the channel.

III. Effective Conduction Path Effect

Considering the polynomial model [11] that consider the conduction current is at the surface of the silicon body and supposes parabolically the electrostatic potential profile in the

$$\varphi(x, y) = C_0(y) + C_1(y)x + C_2(y)x^2 . \quad (10)$$

vertical direction. Using the classical boundary conditions [12]

$$\begin{cases} \varphi(x, y=0) = V_{bi} \\ \varphi(x, y=L) = V_{bi} + V_{ds} \end{cases} \qquad \begin{cases} \left.\frac{\partial \varphi}{\partial x}\right|_{x=0} = \frac{C_{ox}}{\varepsilon_{si}}\left(\varphi(0,y) - \varphi_{gf}\right) \\ \left.\frac{\partial \varphi}{\partial x}\right|_{x=x_m} = 0 \end{cases}$$

and writing the Poisson equation as $\varphi_s(x, y)$, we deduce the polynomial characteristic length

$$\lambda_p = (\varepsilon_{si} x_{max} / C_{ox})^{1/2} . \quad (11)$$

The notion of the ECPE supposes that the gravity center of the conduction current is at $x = d_{eff}$. The presentation of the electrostatic potential $\varphi(x, y)$ at $x = d_{eff}$ allows us to bring about a correction to polynomial characteristic length λ_p. The new corrected characteristic length corresponding to the polynomial model including ECPE is

$$\lambda_{pc} = \lambda_p \left(1 + \frac{C_{ox}}{\varepsilon_{si}} d_{eff} \_1/2 \frac{C_{ox}}{\varepsilon_{si}} \frac{d_{eff}^2}{x_m}\right)^{1/2} \quad (12)$$

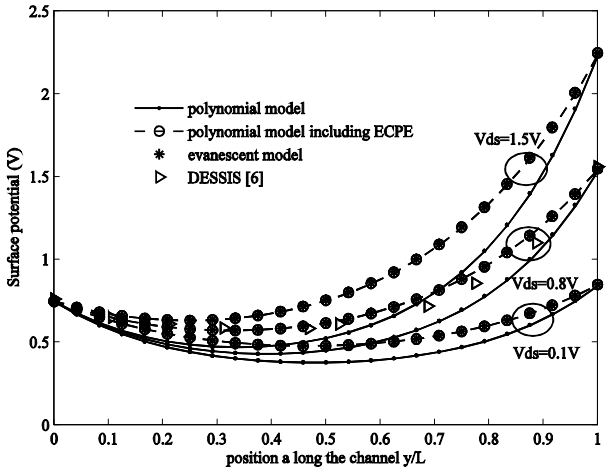

Figure 2. Surface potential versus normalized position a chanel length y/L

The evanescent model and the polynomial model with and without the ECPE are utilized to analysis the short channel effect. The analytic expressions of $\varphi_s, V_{th}, \Delta V_{th}, \Re$ et S presented through the evanescent model remain adequate for the polynomial models with and without ECPE save for the characteristic length $\lambda_{i=e,p,pc}$ which changes in the expressions.

IV. Results and Discussion

We have looked through the convergence of the models studying the short channel effect. The analytic expressions of $\varphi_s, V_{th}, \Delta V_{th}, \Re$ and S are analysis using the models mentioned above. To prove the convergence of the models, some measure of simulators are superposed to the figures of the parameters above.

For the three models, the figure 2 shows the evolution of the surface potential along with the normalized position of the channel length for N_a=6.10^{17}cm^{-3}, T_{ox}=3.5nm, L=80nm and V_{ds}=0.1, 0.8 et 1.5V. We notice that the convergence of the evanescent model and polynomial model including ECPE in a large of scale the drain bias at $d_{eff} = 0.5T_{ox}$. A good agreement, for V_{ds}=0.8V, has been observed between these models and measures of the simulator DESSIS [7].

Figure 3 presents the evolution of the gradient of threshold voltage in regard to the normalized position of the channel length for N_a=1.5.10^{18}cm^{-3}, V_{ds}=1V, L=500nm and T_{ox}=1.5nm and for N_a=3.10^{17}cm^{-3}, V_{ds}=1V, L=500nm and T_{ox}=5nm.

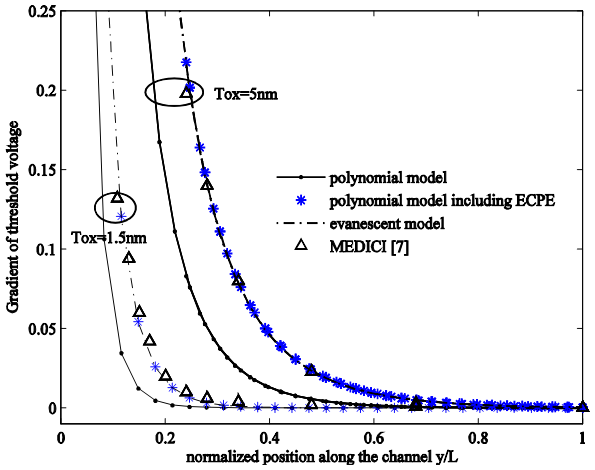

Figure 3. Variation of gradient of threshold voltage versus normalized position along the channel y/L

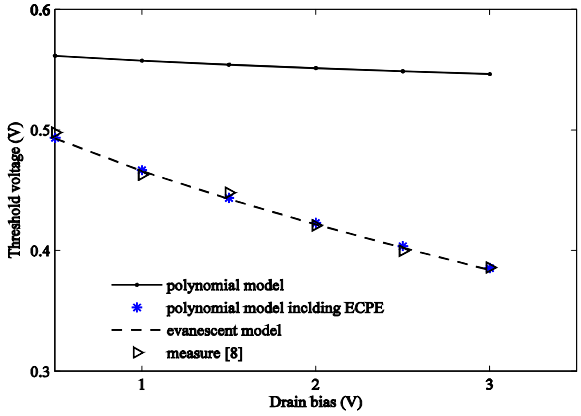

Figure 4. Variation of threshold voltage versus drain bias

We see a good agreement, at $d_{eff} = 0.5T_{ox}$, a between the evanescent model, the polynomial model including ECPE and the measures of the simulator MEDICI [6].

The study of the threshold voltage in regard to the drain bias (V_{ds}) presented in figure 4, displays a good convergence, at $d_{eff} = 0.5T_{ox}$, of the evanescent model, the polynomial model including ECPE and some measure of the reference [8] for N_a=3.6.10^{17}cm^{-3}, T_{ox}=5.5nm and L=0.3µm. The evolutions are almost linear as stated by the model DIBL [13].

The evolution R is reported in figure 5 (for $N_a=3.10^{17}cm^{-3}$, T_{ox}=5.5nm, L=0.5µm and V_{ds}=0.5V) for the three models. A good convergence, at $d_{eff} = 0.5T_{ox}$, has been noticed, along the channel, for the evanescent model and the polynomial model including ECPE.

Figure 6 illustrates the evolution of the parameter S in regard to the channel length for $N_a=1.10^{17}cm^{-3}$, T_{ox}=10nm and V_{ds}=0.1V. The evanescent and the polynomial including ECPE models presents, at $d_{eff} = 0.5T_{ox}$, a good agreement and a little disagreement between these models and the measures of simulator MEDICI [9]. The study of some parameters show a little disagreement between the polynomial model without the ECPE and the others.

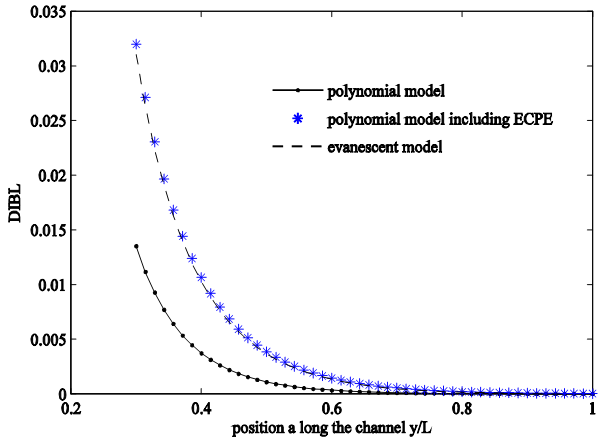

Figure 5. DIBL versus normalized position a channel length y/L

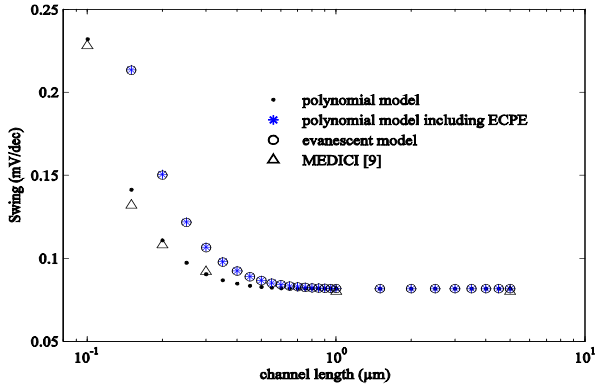

Figure 6. Subthreshold Swing versus a channel length L

V. Conclusion

The short channel effects studied through the surface potential, threshold voltage, DIBL and swing show a good convergence between the evanescent model and the polynomial model including ECPE at $d_{eff} = 0.5T_{ox}$. This agreement of these analytic models is proved by different of 2D simulator.

VI. References

[1] S. H. Oh, D. Monroe and J. M. Hergenrother, "Analytic description of channel effects in fully depleted double gate and cylindrical, surrounding gate MOSFET's", IEEE electron device letters, vol 21, n 9, pp. 445-447, 2000.

[2] H. J. Park, P. K. Ko and C. Hu, "A charge sheet capacitance model for short channel MOSFET's for SPICE", IEEE transactions on computer – aided design, vol 10, n 3, 1991.

[3] A. Aouaj, A. Bouziane and A. Nouaçry, " Analytical 2D modeling for potential distribution and threshold voltage of the short channel fully depleted cylindrical/surrounding gate MOSFET", vol 92, n 8, pp. 437-443, 2005.

[4] J. Lee and H. Shin, " Evanescent mode analysis of short channel effects in MOSFET's", Journal of the Korean Physical Society, vol 44, n 1, pp. 50-55, 2004.

[5] T. K. Chiang, " A new scaling theoriefor fully depleted SOI double gate MOSFET's: including effective conducting path effect (ECPE)", Solid-State Electronics, vol 49, pp. 317-322, 2005.

[6] S. Baishya, A. Mallik and C. K. Sartar, " A threshold voltage model for short channel MOSFET's taking into account the variyng depth of channel depletion layers around the source and drain", Microelectronics Reliability, vol 48, pp. 17-22, 2008.

[7] C. H. Shih, Y. M. Chen and C. Lien, " An analytical threshold voltage roll-off equation for MOSFET by using effective-doping model ", Solid-State Electronics, vol 49, pp. 808-812, 2005.

[8] Z. H. Liu, C. Hu, J. H. Huang, T. Y. Chan, M. C. Jeng, P. K. Ko and Y. C. Cheng, "threshold voltage model for deep-submicro,eter MOSFET's ", IEEE transactions devices, vol 40, n 1, pp. 86-95, 1993.

[9] A. Godoy, J. A. Lopez-Villanueva, J. A. jimenez-Tejada, A. Palma and F. Gamiz, " A simple subthreshold swing model for short channel MOSFET's ", Solid-State Electronics, vol 45, pp. 391-397, 2001.

[10] A. Kumar, T. Nagumo, G. Tsutsui, T. Ohtou and T. Hiramoto, "Body factor conscious modeling of single gate fully depleted SOI MOSFET's for low power applications ", Solid-State Electronics, vol 49, pp. 997-1001, 2005.

[11] V. Aggarwal, M. Khanna, R. Sood, S. Haldar and R. S. Gupta, "Analytical tow-dimentional modeling for potential distribution and threshold voltage of the short channel fully depleted SOI (Silicon On Insulator) MOSFET ", Solid-State Electronics, vol 37, n 8, pp. 1537-1542, 1994.

[12] A. Bouhdada and R. Marrakh, " Modeling of surface potential and threshold voltage of LDD nMOSFET's with localized defects ", Active and Passive Electr. Comp. , vol 23, pp. 61-73, 2000.

[13[1]] D. R. Poole and D. L. Kwong, " Tow-dimentional analysis modeling of threshold voltage of short channel MOSFET's ", vol EDL-5, pp. 443, 1984